Effects of SF_6 Jet-in-crossflow on deflagration-to-detonation transition of premixed methane-oxygen mixture

Jun Cheng, Bo Zhang
Shanghai Jiao Tong University
Shanghai, China

1 Introduction

Detonation propulsion has been considered an advanced propulsion technology and has recently attracted wide attention[1]. Corresponding propulsion devices, such as pulse detonation engines (PDEs), rotating detonation engines (RDEs), and oblique detonation engines (ODEs), have also been proposed in recent decades[2, 3]. However, because of the extremely high ignition energy or the considerable long run-up distance required for the onset of detonation, how to promote flame acceleration and deflagration-to-detonation transition (DDT) is the key problem for engineers to overcome. Recently, the positive effect of turbulence on flame propagation has been proposed and verified by experiments and numerical simulations. Turbulence has been suggested to be able to accelerate DDT, and turbulent generators (e.g., obstacles) have been widely applied in studies of DDT[4, 5]. Flame propagation in obstructed tubes is widely investigated, and it is proposed that the obstacle-induced turbulence could effectively promote flame acceleration and DDT, nevertheless, the obstacle also leads to thrust reduction. To reduce the obstacle-induced flow loss, jet-in-crossflow (JICF) was considered a candidate and was proposed by Knox[6]. McGarry et al.[7, 8] and Peng et al.[9, 10] investigated the effect of JICF on flame propagation experimentally and numerically. The results showed that the JICF-induced mushroom vortices distort the flame surface and increase the flame area, and the perturbation induced by JICF also accelerates shock wave formation. However, the JICF mentioned in recent studies was reactive mixtures or mediums of high combustion intensity; hence, the combustion is enhanced near the JICF. Thus, the effect of turbulence on flame acceleration and DDT cannot be discussed independently.

In our previous work[11], the effect of the mole weight of the JICF medium on the flame transition to deflagration was investigated, and the results showed that the difference in the mole weight of the inert gas and premixed mixture played an important role in flame acceleration. Therefore, SF_6 with a molar weight of 146 was selected as the JICF medium in this study, and its molar weight was nearly 5 times that of the test mixture (i.e., stoichiometric methane-oxygen mixture). Particular attention is given to the behavior of flame evolution affected by SF_6 JICF at different pressure ratios (P_j/P_0). The flame transition and DDT are recorded by the high-speed schlieren system and pressure/ion measurement. The mechanism of flame acceleration and DDT is also explored and discussed.

Correspondence to: bozhang@sjtu.edu.cn

2 Experimental setup

In this study, the experiments were carried out in a rectangular shock tube with a length of 3 m. The schematic of the experimental system is shown in Fig. 1. 9 ion probes (IP1~9) and 5 pressure transducers were utilized to record the time-of-arrival (TOA) of the flame and shock wave, and then to obtain the propagation velocity (v_f, v_s) of the flame and shock wave, respectively. The processes of ignition and earlier flame propagation in the optical window through the JICF were recorded by a high-speed camera (Phantom V710 L) via the schlieren system. The frame rate of the camera was 100 kHz, and the exposure time was 5 μs. Hence, the corresponding flash frequency of the LED light source was 100 kHz as well. SF_6 JICF was controlled by a solenoid valve (FESTO MHE4-MS1H-3/2G-1/4-K), of which the response time (3.5 ms) was much longer than the ignition delay of the premixed mixture; thus, the solenoid valve should be activated before ignition. In this study, the valve worked for 20 ms prior to ignition. The operation times of the solenoid valve and ignitor were 100 ms and 1000 ms, respectively. The initial pressure (P_0) of the methane-oxygen mixture was 20 kPa, and the injection pressure (P_j) of SF_6 JICF ranged from 300 kPa ~ 600 kPa; thus, the corresponding pressure ratio P_j/P_0 was 15~30. The detailed experimental sets were listed in Table. 1.

Table. 1 Details of the experimental conditions in this study

Case	Medium	P_j/kPa	P_j/P_0
0	-	-	-
1	SF_6	300	15
2		400	20
3		600	30
4	He	300	15
5		400	20
6		600	30
7	N_2	300	15
8		400	20
9		600	30

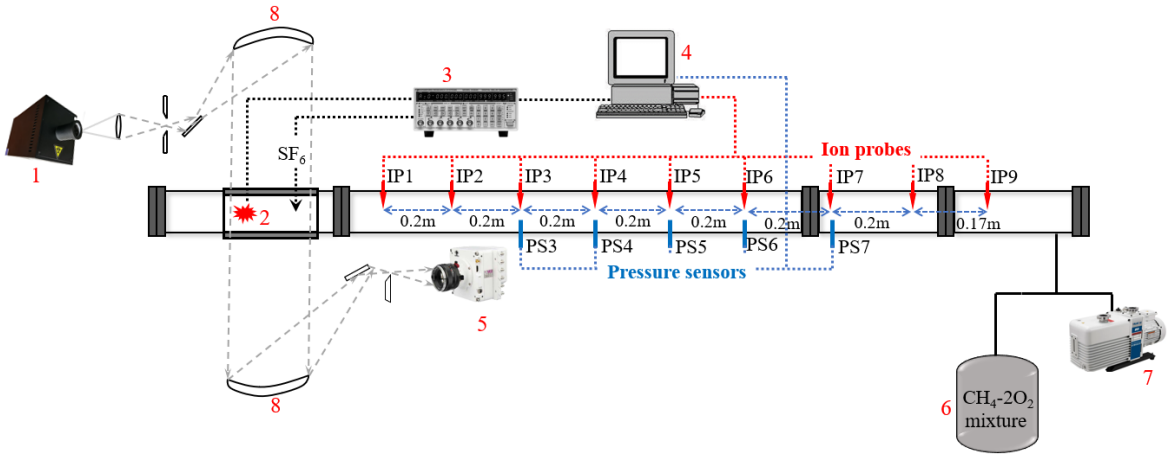

Fig. 1. The experimental system (1: LED light source; 2: Electrode ignitor; 3: Digital delayer; 4: Computer for signal control and data collection; 5: High-speed camera; 6: Premixed chamber; 7: Vacuum pump; 8: Schlieren mirror)

3 Results and discussion

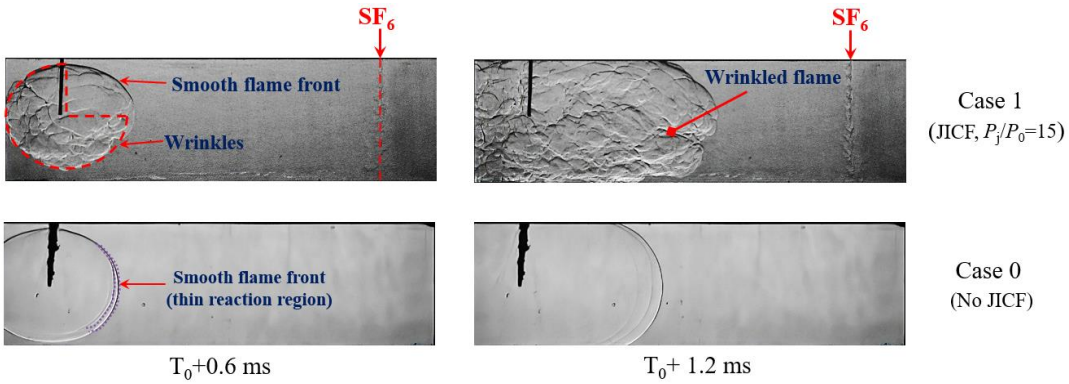

Fig. 2 The flame details of Case 1 and Case 0 at (T_0+0.6) ms and (T_0+1.2) ms

Fig. 2 shows the flame details of the two cases at (T_0+0.6) ms and (T_0+1.2) ms. At (T_0+0.6) ms, for Case 0, the flame expands uniformly, and the flame front propagates spherically. The flame area is smooth, and the reaction only occurs at the thin flame front highlighted by purple dotted lines. In Case 1, there are some wrinkles inside the flame, and the wrinkled part of the flame propagates slightly slower than the smooth part of the flame because of the combustion-inhibition effect of SF_6 deposited near the bottom wall. The upper part of the flame surface has few wrinkles, which indicates that the combustion-inhibition effect of SF_6 is weak near the upper wall. At (T_0+1.2) ms, the flame in Case 1 has been entirely wrinkled, while the flame in Case 0 remains smooth. The flame area of Case 1 is larger than that of Case 0, and the position of the flame front of Case 1 is also ahead of that of Case 0. Hence, it is suggested that the area of the disturbed flame increases and reactions on the flame are enhanced, resulting in a significant heat release increase that promotes flame acceleration. SF_6 JICF shows two aspects of effects on flame propagation. On the one hand, SF_6 dilutes the premixed combustible mixture and suppresses the reaction on the flame; on the other hand, vortices induced by SF_6 JICF could increase the turbulence intensity of the background flow field, and the entertainment effect of vortices also stretches the flame surface to increase the flame area and accelerate flame propagation. Fig. 3 compares the nondimensional propagation velocity of the precursor shock wave (solid lines) and the flame (dashed lines) of the aforementioned two cases. Apparently, the deflagrated flame could transit to detonation within a short run-up distance (~1.25 m) by the SF_6 JICF-induced disturbance.

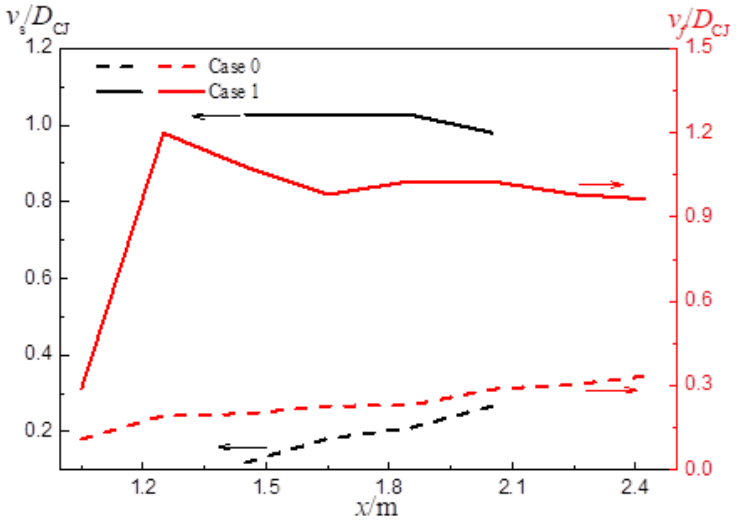

Fig. 2 The propagation velocity of the precursor shock wave (v_s) and flame (v_f) in Case 0 and 1

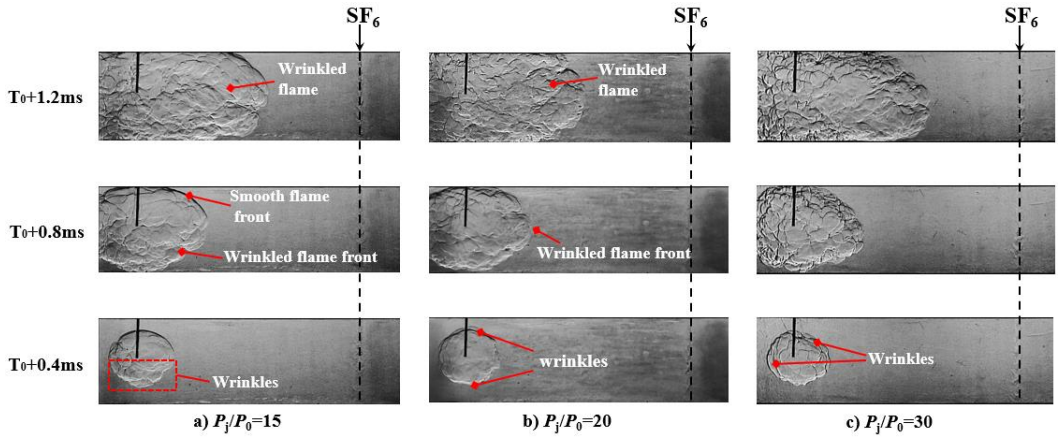

Fig. 3 Details of the flame evolution of Case 1, 2 and 3

Fig. 3 shows the details of the flame in Case 1, 2, and 3 at three moments. At (T_0+0.4) ms, when the flame is perturbed by the SF_6 JICF of low injection pressure in Case 1, wrinkles first mainly appear inside the lower part of the flame, while there are a few wrinkles inside the upper part. Meanwhile, for Case 2 and 3, it is found that the wrinkles first appear on the flame front, especially for the flame disturbed by SF_6 JICF of P_j/P_0=30, wrinkles occupy the flame front and the flame front cannot sustain smoothness. It is noted that there are few wrinkles formed inside the flame in Case 2, while there are a few wrinkles inside the flame in Case 3. At (T_0+0.8) ms, in all three cases, wrinkles fill up the whole flame area, and the wrinkles are much more serried in Case 3. The wrinkles in the cases with SF_6 JICF of P_j/P_0=15 and 20 remain concentrated in the lower part of the flame and flame front, respectively. There are also a few wrinkles distributed in the upper part of the flame in both cases. It is noteworthy that the wrinkles spread throughout the whole flame rapidly in Case 3. In addition, in Case 3, the wrinkles are clearer and smaller than those in Case 1 and 2. At (T_0+1.2) ms, the positions of the flame front in Case 1 and 3 are slightly ahead of that in Case 2, which means that the flame propagates faster in Case 1 and 3. At this moment, the flames in the three cases are entirely wrinkled. The distribution and scale of the wrinkles on the flame of the three cases are similar to the previous moment. In general, as P_j/P_0 increases, the mass of SF_6 injected into the tube increases as well as the injection velocity. Hence, the diffusion and turbulent effects are more complex, which enhances the dilution degree of the premixed mixture and the stretching effect on the flame surface. Fig. 4 presents the nondimensional flame propagation velocity (v_f/D_{CJ}) along the tube measured in Case 1-3. Apparently, for the three cases disturbed by SF_6 JICF of different P_j/P_0, the flame has a coincident propagation process along the tube.

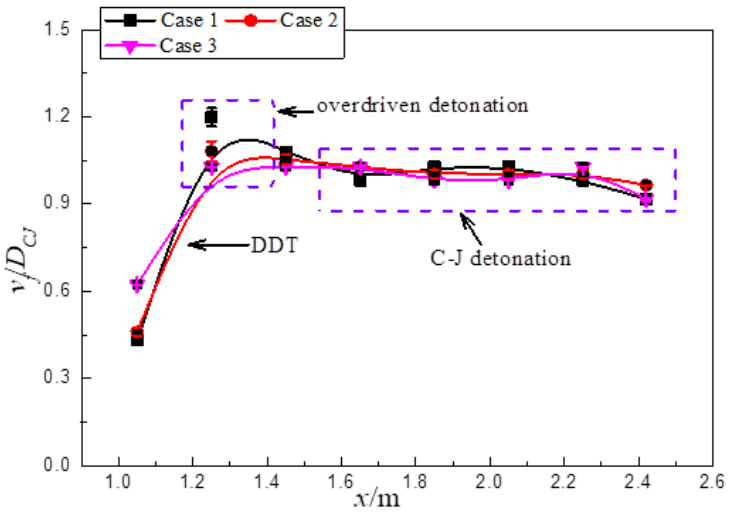

Fig. 4. Comparison of the flame propagation velocity in the cases of different P_j/P_0

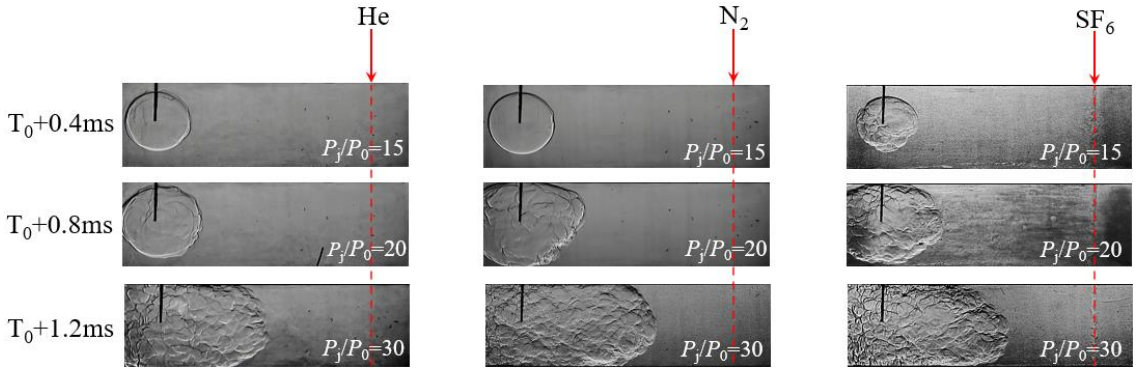

Fig. 5. The evolution of the flame disturbed by different JICFs

Fig. 5 presents the flame evolution in the schlieren window in the cases with different inert gas JICFs. At (T_0+0.4) ms, it is apparent that the flame disturbed by the He and N_2 JICF is relatively smooth compared with the flame affected by the SF_6 JICF. In the case with He JICF (Case 4), only a few wrinkles form at the upper flame front. In the case with N_2 JICF (Case 7), the flame remains smooth, and there are no wrinkles at the flame front. At (T_0+0.8) ms, different from the flame in the case with SF_6 JICF (Case 2), wrinkles concentrate in the upper part of the flame in the cases with He (Case 5) and N_2 JICF (Case 8). He (helium) mainly floats in the upper part of the tube because it is lighter than the methane-oxygen mixture; thus, it could be moved to the upper wall by Rayleigh-Taylor instability. At (T_0+1.2) ms, wrinkles are distributed homogeneously in the flame of the case with He JICF (Case 6). In the case with N_2 JICF (Case 9), the wrinkles are smaller than those of Case 6, whereas their distribution is relatively homogeneous as well. Apparently, compared with Case 6 and 9, the wrinkles in Case 3 are the smallest and the most densely distributed.

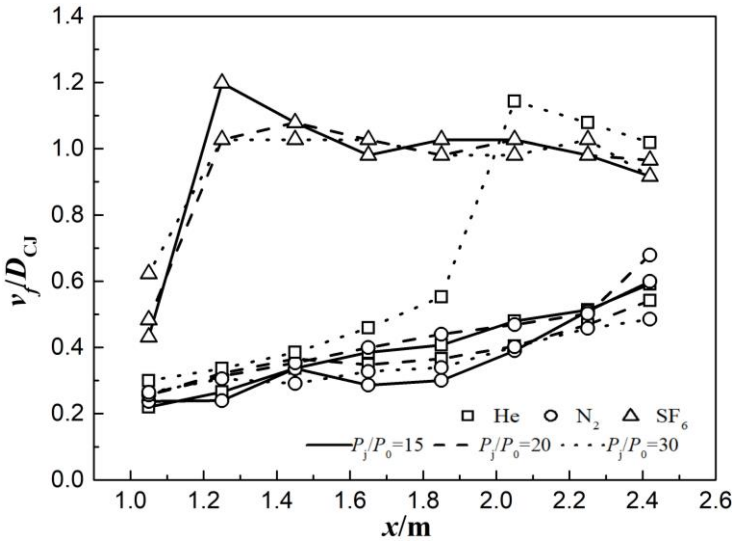

Fig. 6. The nondimensional flame propagation velocity along the tube

Fig. 6 compares the nondimensional flame propagation velocity along the tube in the cases with different JICFs. In the cases with SF_6 JICF of different pressure ratios, it is apparent that the flame accelerates significantly at x=1.05 m and then transits to an overdriven detonation at x=1.25 m. The flame subsequently propagates at a speed of 0.95 D_{CJ} along the tube, which demonstrates that the overdriven detonation finally decays to C-J detonation. However, in the cases with N_2 JICF, the flame propagation velocity only increases to 0.5 D_{CJ} finally. The final flame propagation velocities affected by He JICF of

P_j/P_0=15 and 20 are 0.6 D_{CJ} and 0.4 $D_{CJ,}$ respectively, whereas the flame of the case with He JICF of P_j/P_0=30 transits to overdriven detonation successfully at x=2.05 m and then decays to C-J detonation. Thus, compared with He and N_2 JICF, SF_6 JICF could significantly promote the flame transiting to detonation and shorten the run-up distance to the onset of detonation.

4 Conclusions

The main conclusions of this study could be summarized as follows:

(1) SF_6 JICF could effectively promote flame acceleration and shorten the run-up distance of the onset of detonation.

(2) Increasing P_j/P_0 of SF6 JICF could affect the flame evolution, whereas it shows no significant further improvement in the acceleration of DDT.

(3) Compared with He or N_2 JICF, SF_6 JICF shows the best performance in promoting flame acceleration and DDT.

References

[1] D.A. Rosato, M. Thornton, J. Sosa, C. Bachman, G.B. Goodwin, K.A. Ahmed, Stabilized detonation for hypersonic propulsion. Proceedings of the National Academy of Sciences 20118 (2021).

[2] M.N. Nejaamtheen, J. Kim, J. Choi, Review on the research progresses in rotating detonation engine, Springer, 2018, pp. 109-159.

[3] R. Yokoo, K. Goto, J. Kim, A. Kawasaki, K. Matsuoka, J. Kasahara, A. Matsuo, I. Funaki, Propulsion performance of cylindrical rotating detonation engine. Aiaa J. 1258 (2020) 5107-5116

[4] M. Cooper, S. Jackson, J. Austin, E. Wintenberger, J.E. Shepherd, Direct experimental impulse measurements for detonations and deflagrations. J. Propul. Power 518 (2002) 1033-1041.

[5] X. Sun, S. Lu, Effect of obstacle thickness on the propagation mechanisms of a detonation wave. Energy 198 (2020) 117186.

[6] B. Knox, D. Forliti, C. Stevens, J. Hoke, F. Schauer, A comparison of fluidic and physical obstacles for deflagration-to-detonation transition, 2011, p. 587.

[7] J.P. McGarry, K.A. Ahmed, Flame-turbulence interaction of laminar premixed deflagrated flames. Combust. Flame 176 (2017) 439-450.

[8] J.P. McGarry, K.A. Ahmed. Laminar deflagrated flame interaction with a fluidic jet flow for deflagration-to-detonation flame acceleration. In 51st AIAA/SAE/ASEE Joint Propulsion Conference. 2015: 4096.

[9] H. Peng, Y. Huang, R. Deiterding, Z. Luan, F. Xing, Y. You, Effects of jet in crossflow on flame acceleration and deflagration to detonation transition in methane-oxygen mixture. Combust. Flame 198 (2018) 69-80.

[10] H. Peng, Y. Huang, R. Deiterding, Y. You, Z. Luan, Effects of Transverse Jet Parameters on Flame Propagation and Detonation Transition in Hydrogen–oxygen-argon Mixture. Combust. Sci. Technol. 9193 (2021) 1516-1537.

[11] J. Cheng, B. Zhang, H. Liu, F. Wang, Experimental study on the effects of different fluidic jets on the acceleration of deflagration prior its transition to detonation. Aerosp. Sci. Technol. 106 (2020) 106203.